Shearing a glass and the role of pinning delay in models of interface depinning

Stefanos Papanikolaou

Phys. Rev. E **93**, 032610 — Published 24 March 2016

DOI: 10.1103/PhysRevE.93.032610

Shearing a glass and the role of pin-delay in models of interface depinning

Stefanos Papanikolaou[1,2]

[1]*Department of Mechanical Engineering, The Johns Hopkins University, 3400 N Charles St, Baltimore, MD, 21218*
[2]*Hopkins Extreme Materials Institute, The Johns Hopkins University, 3400 N Charles St, Baltimore, MD, 21218*

When a disordered solid is sheared, yielding is followed by the onset of intermittent response that is characterized by slip in local regions usually labeled shear-transformation zones (STZ). Such intermittent response resembles the behavior of earthquakes or contact depinning, where a well-defined landscape of pinning disorder prohibits the deformation of an elastic medium. Nevertheless, a disordered solid is evidently different in that pinning barriers of particles are due to neighbors that are also subject to motion. Microscopic yielding leads to destruction of the local microstructure and local heating. It is natural to assume that locally a liquid emerges for a finite timescale before cooling down to a transformed configuration. For including this characteristic transient in glass depinning models, we propose a general mechanism that involves a "pin-delay" time T_{pd}, during which each region that slipped evolves as a fluid. The new timescale can be as small as a single avalanche time-step. This is a local, effective and dynamical in nature, mechanism that may be thought as dynamical softening. We demonstrate that the inclusion of this mechanism causes a drift of the critical exponents towards higher values for the slip sizes τ, until a transition to permanent shear-banding behavior happens causing almost oscillatory, stick-slip response. Moreover, it leads to a proliferation of large events that are highly inhomogeneous and resemble sharp slip band formation.

Extreme phenomena in nature appear in a wide range of scales, from the abrupt nano-deformation of materials to earthquake faults that extend several miles. At all scales, avoiding such phenomena requires a deep understanding of the disparate timescales leading to separate as well as collections of events. Material plastic deformation displays characteristic intermittency in a wide range of systems: single crystals [1], bulk metallic glasses (BMG) [2–4], disordered granular solids [5, 6], colloids [7], frictional contacts [8, 9]. While numerical simulations of materials can be very detailed at short timescales, the detailed study of a collection of abrupt events remains still out of reach. The theoretical intuition for such systems comes from the thorough study of *interface depinning*: a d-dimensional elastic string travelling on a landscape of quenched disorder in $d+1$ dimensions under the help of a uniform external force [10]. In complex disordered solids, though, while the assumption of an elastic medium appears reasonable, the one related to quenched disorder should be placed under scrutiny: Pinning disorder for every particle originates in the actual interface that attempts to depin (other nearby particles); a disordered solid pins itself during deformation. A basic consequence is that local glass depinning is not *immediately* followed by re-pinning; instead, in short-time transients (compared to typical avalanche durations), the system behaves locally as a fluid of finite viscosity η; the timescale for such fluid-like transients should not necessarily be at the particle motion timescale – instead, it should correspond to the timescale for the system to traverse through local metastable minima before ultimately reaching the global metastable minimum. In a sense, this timescale should be proportional to the number of steps needed to reach each metastable minimum in a quasi-static steepest-descent algorithm. In the context of depinning models we call this phenomenon *pin-delay*, generalizing the concept of complex fluid *thixotropy* [11]: the change from a solid-like elastic gel to a flowable fluid as a function of time at fixed external stress. Thixotropy in fluids deeply originates in the chainy/anisotropic and hard-core/impenetrable nature of the local degrees of freedom/molecules: We conjecture that it is this kind of anisotropy that can lead hard-core systems to develop shear-band phenomena. In this paper, we focus on

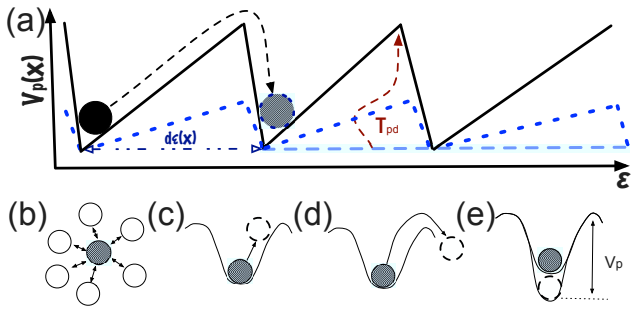

FIG. 1: **Thixotropic effects in depinning modeling**. Lower panel shows schematics how different mechanical states can be viewed in terms of their local potential well. Viscoelasticity brings particles back to their minima after the removal of the external stress, while in a liquid particles jump away from their minima. Thixotropy corresponds to the curious case where the minimum becomes deeper with time. Such a phenomenon is pronounced in materials that are composed of highly anisotropic/chainy molecules. Depinning is thus a liquid form; to add thixotropy, minima should become deeper after yielding. Upper panel shows a typical random pinning potential for a single interface location $V_p(\mathbf{x})$ as a function of plastic strain, as it is used in simulations. As external force increases, the interface slips by $d\epsilon(\mathbf{x})$, the pinning potential disappears and then It reappears thixotropically (dashed lines) to its parent form during time T_{pd}. We consider, in simulations, the simplest case where at time T_{pd} the potential appears in a single step.

the problem of plastic deformation in disordered solids and we investigate how pin-delay influences the statistics of avalanches and global strain behavior in a simple model. We show that the pin-delay effect drastically leads to shear-banding without explicitly considering local anisotropy. We conjecture that local potential anisotropy which is abundant in thixotropic fluids, should be also observable in other disordered solids in their flowing mesoscale state.

Plastic deformation in disordered solids, such as BMGs or granular piles, has been a topic of interest for several decades [12–15]; recently, it has become clear in well controlled experiments that it does not evolve smoothly but through plastic bursts that organize into stick-slip stress oscillations with universal scaling [5]. In a paradox, *strongly disordered* solids display plastic bursts along STZs [16] that spatially organize along *strongly ordered* sharp (nanometer-range) slip bands, a phenomenon coined *slip localization*. In simulations, avalanche statistics in both two and three dimensions [17] display universal behavior [19, 20] with the critical exponent $\tau \simeq 1.3$ if the particle ensemble follows steepest-descent dynamics. That universality class appears to be consistent with a simple, coarse-grained model of interface depinning [21, 22]. In retrospect, for less dissipative dynamics, Salerno and Robbins [17] reported in both two and three dimensions a crossover where the stress drops display different universal statistics with $\tau \simeq 1.6$ and larger and strongly anisotropic plastic bursts [23].

Overdamped dynamics has been essential in the study of avalanche critical behavior, since it facilitates the definition of events' start and end points, as well as correlates with some experimental evidence, especially in granular systems' dynamics. Departing away from that assumption to more complex local dynamics, such as underdamped finite inertia dynamics or thixotropic aging, is typically avoided. Finite inertia carries a system over successive (in deformation) pinning-potential energy minima to *minimize elastic interactions* and its effect appears similar to thixotropy, in essence. The common approach used to include such, still over-damped, effects is through emulating a frictional stick-slip mechanism, with rules that lower pinning barriers after the initial slip [24–29], without successive minima jumps or direct elastic interaction minimization of any sort. All studies of this type find that addition of local weakening introduces a global stick-slip instability discontinuously [25, 26, 29, 30]. Another approach to model such effects is through the inclusion of viscous effects in the elastic interaction, however the behavior is questionable near the depinning transition [48]. Finally, in mean-field approaches of interface depinning it is possible to study effective acceleration terms, but they do not alter the critical exponents and qualitative behavior near depinning [31].

In this paper, we propose a mechanism to introduce such weakening memory-effects through which abrupt local slip leads to the disappearance of the local pinning potential for a characteristic timescale T_{pd}. This is a local thixotropic feature that we conjecture to be present in all disordered solids, independent of composition or scale of fluctuations. During the interval T_{pd}, the system *flows* locally as a fluid of viscosity η (considered a material property that can be thought as an analog of Newtonian fluid viscosity, but defined for transients between slip events). This mechanism is a dynamical weakening effect that may be present in systems which are characterized by strongly anisotropic interactions and hard-core effect frustrations (the basic features of thixotropic fluids). The dynamical nature of this weakening should be contrasted to typical friction-related weakening effects that generically appear in analogous studies. [25, 26, 29, 30] In our model, weakening and aging effects are directly inter-connected, in contrast to friction-related investigations.

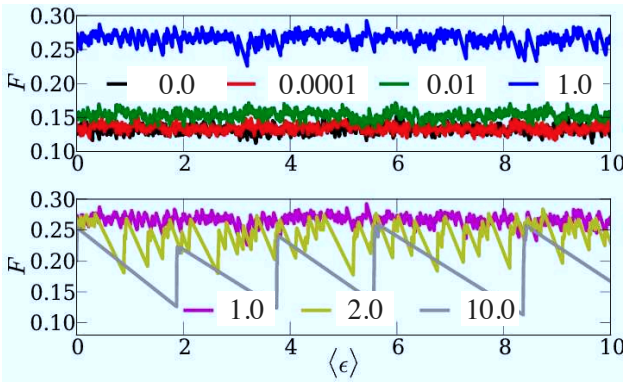

FIG. 2: **Effect of D on serrated flow distributions**. We set $L = 128$ and $T_{pd} = 8$. The evolution of serrated flow structure is shown as D increases. When $D < D^*$, its increase leads to a flow stress increase, due to competing effect of the relaxation. When $D > D^*$, stick-slip behavior is observed.

We follow Talamali *et al.*'s approach [21] for $d = 2$ systems and assume that plastic deformation in disordered solids is modeled by the $xx-$component of the strain tensor $\epsilon \equiv \epsilon_{xx} = -\epsilon_{yy}$. The interaction due to local slip is the stress generated by local deformations of a random medium [32], which takes the form $\tilde{F}_{\rm int}(k,\omega) = (-\cos(4\omega) - 1)\tilde{\epsilon}$ where k, ω are the polar coordinates in Fourier space [34] and $\tilde{\epsilon}$, $\tilde{F}_{\rm int}$ are the transforms of the interaction and the strain. We scale the interaction strength by $c = 0.1$, equivalent to modifying the strain-slip scale. We initialize the $L \times L$ system with $\epsilon(\mathbf{x}) = 0\ \forall\ \mathbf{x}$ and stress thresholds $f_p(\mathbf{x})$ taken from a uniform distribution $[0, 1)$. We increase the external stress F quasistatically until yielding, and then, the following evolution equation is solved,

$$\frac{d\epsilon(\mathbf{x})}{dt} = \sigma(\mathbf{x}) = F_{\rm int}(\mathbf{x}) + F - f_p(\mathbf{x}) - \tilde{k}v(\mathbf{x}) \qquad (1)$$

Assuming that $f_p(\mathbf{x})$ corresponds to a pinning potential resembling the one in Fig. 1 (upper panel), we implement a simple algorithm to integrate the above equa-

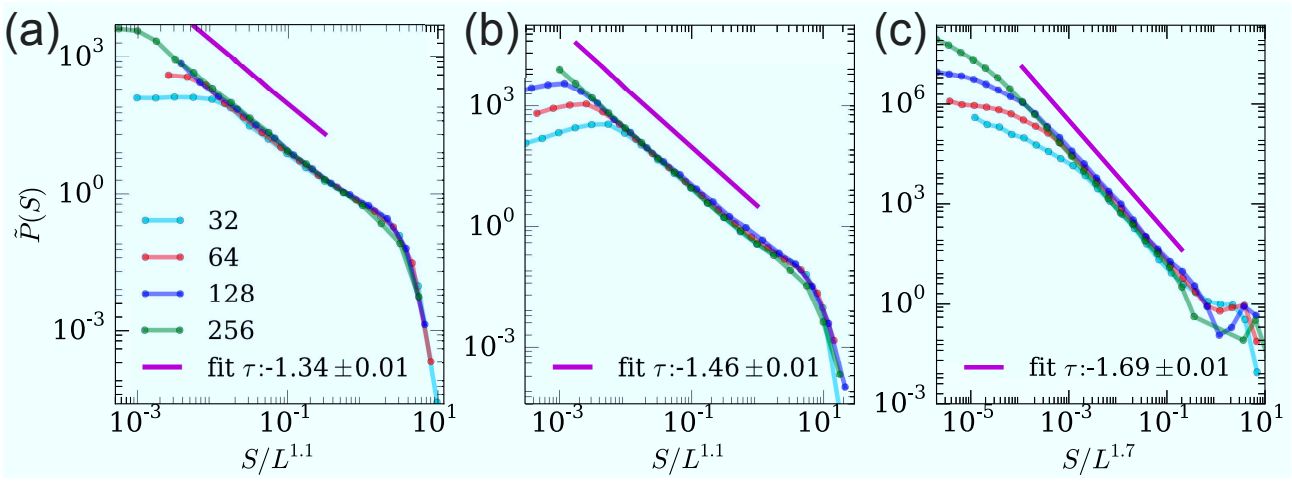

FIG. 3: **Scaling collapses of slip size probability distributions**. Size distributions are shown at $D = 10^{-5}, 10^{0}$ and 10^{1} at $T_{pd} = 8$, $\tilde{k} = 0.2$. At high D, there is a clear drift of the critical exponent τ to ~ 1.7, the cutoff scaling exponent also changes from ~ 1.1 to ~ 1.7 and the shape of the scaling function is clearly modified with an observable hump at large sizes.

tion, in that there is a strain increase $d\epsilon(\mathbf{x})$ randomly picked from a uniform $[0, 1)$ distribution (characteristic of the pinning potential) when $\sigma(\mathbf{x}) > 0$. The stress is decreased by $\tilde{k}v(\mathbf{x})$ at each time-step, where $\tilde{k}$ is a local material weakening parameter and $v(\mathbf{x})$ represents the fraction of STZs that yielded at the previous time-step. [49] The term $\tilde{k}v(\mathbf{x})$ is common in depinning phenomena of disordered magnets and implies a demagnetizing effect due to a response from the material boundary [44]. In the case of disordered solids (BMGs or granular materials) it is common in terms of a phenomenological dilatation effect that reduces the flow. Dilatation, viewed as a reduction of solidity, has two principal effects from a depinning viewpoint: First, the flow rate is reduced; Second, effective pinning weakens for a brief time interval. Thixotropic effects (*cf.* Fig. 1 (lower panel)) describe the latter effect, and can be implemented in the following way: for every element $\mathbf{x}$ that slipped at time t, we demand that $f_p(\mathbf{x}) = 0$ for a pin-delay time-interval T_{pd} that is an integer multiple of the unit time-step in an avalanche. Then, in the simplest possible ansatz, during the pin-delay time after the slip, the system locally evolves as a fluid, assuming a fluidity coefficient $D \equiv 1/\eta$,

$$\frac{d\epsilon(\mathbf{x})}{dt} = D\,\sigma(\mathbf{x}) \tag{2}$$

When time T_{pd} has lapsed or the avalanche stops, a random thresholding force is picked. The avalanche stops when $\sigma(\mathbf{x}) < 0\ \forall\ \mathbf{x}$.

We first investigate this model as a function of $D \equiv 1/\eta$ for fixed $T_{pd} = 8$. The external stress required to maintain the steady state behavior starts decreasing and develops stick-slip oscillations as $D > D^* \simeq 1$ (*cf.* Fig. 2, D^* is defined through the instability towards). The critical exponent τ for the power law behavior of the slip size distribution increases from ~ 1.3 [34] to ~ 1.52 (and up to $1.65 - 1.7$ for $D > 1$) and the form of the universal scaling function acquires a large-event hump (*cf.* Figs. 3, 4). It is possible to perform a scaling collapse for the two different regimes at small and large D (*cf.* Fig. 3): the behavior stays universal but the cutoff S_0 scales differently with the system size, $\sim L^{1.1}$ at low D and $\sim L^{1.7}$ at high D. For intermediate $D \simeq D^* \simeq 1$, we observe a smooth exponent crossover. Avalanche durations (which are directly proportional to the stress drops in this model) display analogous behavior with their critical exponent changing from 1.6 to 2.1 and their cutoff exponent also changes from ~ 1.15 to ~ 1.7. For a scaling distribution $P(S) \sim S^{-\tau}$, that is trivially normalized $\int P(S, L)dS = 1$, one has $\tilde{P}(S) \equiv L^{\alpha}P(S) = g(S/L^{\alpha})$. Finally, we mention that at large D the scaling collapse is not complete (the functional form at the cutoff region weakly changes) because an additional variable is present in the scaling function, $\tilde{k}$. The decrease of $\tilde{k}$ leads to a hump at larger sizes (*cf.* Fig. 4(b)) and with the current definitions, keeping $\tilde{k}$ fixed implies positive scaling of the average avalanche size with the system size [21]; thus, larger system sizes are closer to the parent depinning critical point; if we hold the distance from the critical point fixed (*ie.* by modifying $\tilde{k}$ to keep $\langle S \rangle$ fixed as the system size increases at $D = 0$) then a multi-variable scaling collapse is possible, in the spirit of previous work on models of interface depinning [36].

It is interesting that the two different regimes compared to D^* can be understood through an order parameter, the amount of slip that took place during relaxation (Eq. 2) in comparison to the net slip (the sum of the result of Eqs. 1 and 2). The ratio of the relaxation slip over the net slip seems to display a strong increase from ~ 0 at $D \simeq D^*$, and the increase becomes more drastic as $\tilde{k}$ is smaller (*cf.* Fig. 5). The behavior of this ratio with D suggests that the new $D > D^*$ regime is charac-

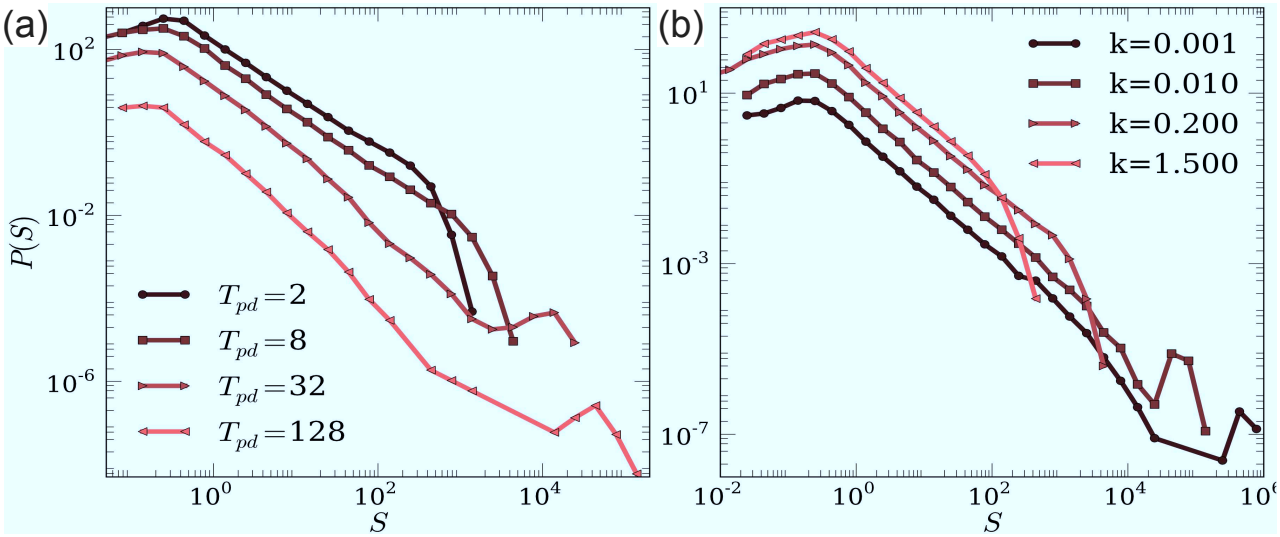

FIG. 4: **Effect of T_{pd} and k on serrated flow distributions**. a. The increase of T_{pd} leads to exponent increase, and behavior that resembles the large D behavior. Here $D = 0.1$, $\tilde{k} = 0.2$. b. The increase of $\tilde{k}$ ($T_{pd} = 8$, $D = 0.2$) leads to reduction of the cutoff size. Distributions are shifted by factors of 4 for clarity.

terized by deformation, filled with spanning events, that displays a discontinuity as function of the driving force F. D^* displays a dependence on $\tilde{k}$ and T_{pd} which qualitatively resembles a scaling relation $D^* \sim \tilde{k}^\theta / T_{pd}^\eta$ with $\theta \simeq 1$ and $\eta \simeq 2$ (*cf.* Fig. 4); however, the precise form of this dynamical transition surface requires further investigation and lies beyond the purpose of this work.

For the behavior as a function of T_{pd} for fixed D, we find that at low $D < D^*(\tilde{k}, T_{pd})$, the increase of T_{pd} leads to smaller avalanches following the same parent distribution and similar critical exponents, acting in a sense like increasing $\tilde{k}$. However, the strength of D is too small to build correlations among different STZs and thus, the critical exponents remain unaltered. However, as $D > D^*(\tilde{k}, T_{pd})$ (*cf.* Fig. 4(a)) the increase of T_{pd} leads to larger avalanches, higher exponent τ (up to ~ 1.7) and a hump in the probability distribution that grows as $\sim 1/\tilde{k}$.

When $\tilde{k}$ decreases, independently of the value of D, there appears to be a consistent drift of the exponent τ towards higher values, but the scaling function displays the characteristic hump (*cf.* Fig. 4(b)), and in that regime the critical exponents change drastically. The avalanche sizes at the hump scale as $\sim 1/\tilde{k}$ and it appears plausible to conjecture that for any D there is a small enough $\tilde{k}$ below which stick-slip behavior emerges, given the dynamical nature of the weakening effects. Analogous dynamical-weakening-induced stick-slip behavior has been also suggested in terms of crystal plasticity aging mechanisms that led to the characterization of avalanche oscillators. [37].

The $D > D^*(\tilde{k}, T_{pd})$ regime is not critical in that it is dominated by spanning events, it corresponds to the "moving phase" in interface-depinning language for *any* stress. This is an expected outcome, since for large D, slow relaxation or creep overcomes any tendency for avalanches, so for any stress there is smooth flow in the system. It is only for small D that there is a transition as a function of stress, from small events ("pinned" phase) to large ones ("moving"). However, since the weakening mechanism presented here is truly dynamical in nature, the off-critical exponent of the small-event distribution is strongly influenced by the dynamical mechanism in the presence of the spanning events.

Large events at the hump of the distributions, at large D, display a non-trivial system-spanning anisotropy along the diagonals, resembling sharp slip band formation (*cf.* Fig. 6(c)), in a strong amplification of the anisotropic features at $D = 0$ [21] (see also Fig. 6(a)). The features of Fig. 6 (right) are qualitatively independent of short-range features of the interaction, since they persist in the presence of a small-amplitude laplacian/diffusion term in the interaction ($\sim k^2$). The pin-delay mechanism appears as a possible candidate to explain the onset of sharp shear bands in disordered solids under shear, as the strain profile is driven towards anisotropy as well (*cf.* Fig. 4(d)) in a consistent, discontinuous manner. It is worth noting that there are several suggestions for the onset of slip bands related to slow structural relaxations [38, 39]. Most of existing mechanisms correspond to a local weakening effect – here, the weakening is dynamical in nature and comes out of a balance of strengthening and weakening in spatially separated regions, through long-range mutual stress interactions.

The "pin-delay" mechanism in models of interface depinning is generally applicable. It is possible to formally introduce the "pin-delay" mechanism in depinning models by redefining the pinning term's strength

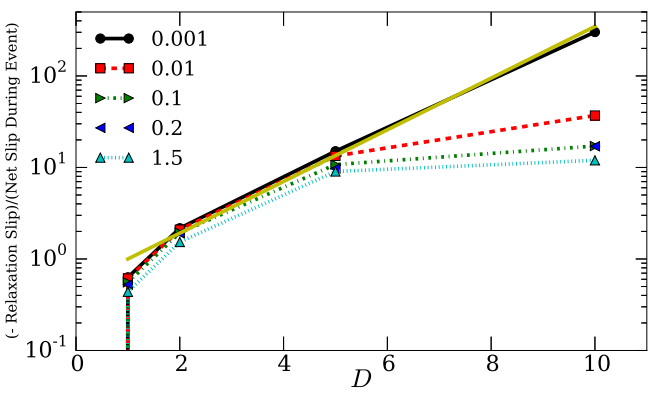

FIG. 5: **Effect of D on serrated flow distributions**. We set $L = 128$ and $T_{pd} = 8$. The fraction of slip during relaxation compared to net slip is shown. A transition is clear at $D \simeq D^* \simeq 1$, where the net slip is a clear outcome of the competition between relaxation and avalanches. Different plots correspond to different $\tilde{k}$. The fit, for $\tilde{k} \to 0$, of the plot to an exponential gives our estimate for D^*. The yellow line (color online) corresponds to such an exponential fit. Increasing the system size L plays an important role on the small D deviations from the fit.

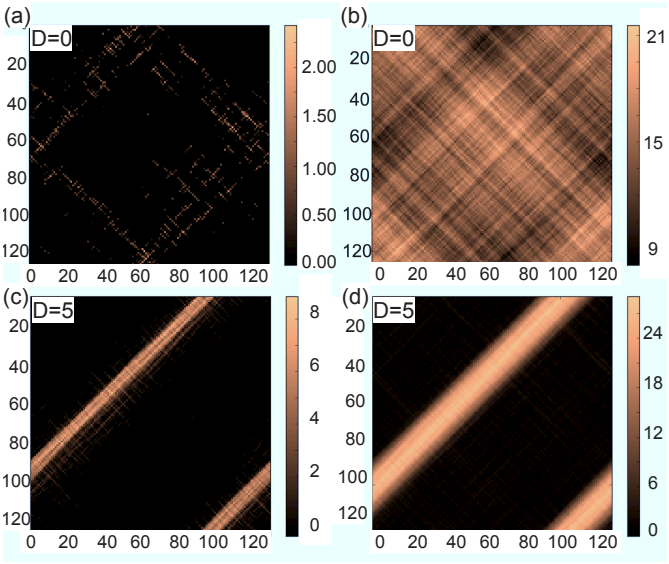

FIG. 6: **Shear band formation due to pin-delay**. Here $L = 128$, $\tilde{k} = 0.2$, $T_{pd} = 8$. The avalanche slip strain is shown on the left due to a typical large event near the cutoff of the distributions. The two dimensional strain-profile is shown on the right at the same strain as the one for the event shown. **Upper:** For small D, there are large events (left) but they appear non-spanning and not leading to shear-band formation [21]. **Lower:** Large events lead to shear-band formation in the strain profile. Large events at the hump location of the avalanche size distribution display sharp slip-band formation that is spanning along the diagonal, with thickness that decreases with system size. Our results are unaffected by a small diffusion term added to the elastic interaction for regularizing short-range interaction effects.

$f_p(\mathbf{x}) = -\partial V_p(\epsilon)/\partial\epsilon(x)$ (*cf.* Fig. 1), which is traditionally time-independent in such a way that adds a specific time-dependence. In our model, $f_p \to C_{pd}(t) f_p$ (where f_p is a typical random-pinning force, satisfying a typical random distribution, as in typical interface-depinning models) with $C_{pd}(t) = \frac{1}{T_{pd}} \int_{-\infty}^{t} dt' e^{-(t-t')/T_{pd}} (1 - \Theta(\dot{\epsilon}(\mathbf{x}, t') - v_{th}))$ or $C_{pd}(t) = \prod_{t'=t-T_{pd}}^{t} (1 - \Theta(\dot{\epsilon}(\mathbf{x}, t') - v_{th}))$ (the latter applies directly to the model numerically solved in this paper) and the pinning term [10] is multiplied by $C_{pd}(t)$, while all other stress terms are multiplied by $C_{pd}(t) + 1/\eta(1 - C_{pd}(t))$. When the system locally slips $\dot{\epsilon} > v_{th}$ (where v_{th} is a threshold for viscoplastic flow rates), it locally flows with viscosity η for time T_{pd} to minimize the local stress with no pinning force present. After the timescale T_{pd}, usual pinning forces develop, derived by a local pinning potential such as in Fig. 1.

Molecular dynamics simulations of disordered particle configurations in Refs. [17, 23], showed that disordered solids undergoing underdamped dynamics enter a regime where τ appears to show a crossover from ~ 1.3 to ~ 1.6, estimated through the careful investigation of stress drops. This exponent crossover together with qualitative features (hump) of the identified scaling function resemble the behavior of our model. However, in those simulations, system-spanning events were not clearly identified – possibly suppressed due to simulational artifacts. Our work suggests that system-spanning events are a clear characteristic of this phase. Our model suggests an apparent resemblance with the features of those simulations: The exponent that characterizes the scaling of the distributions' cutoff S_0 with the system size (Salerno *et al.* [17] also label it α) drifts from ~ 0.9 to ~ 1.6 in the underdamped regime; it resembles the drift observed here for the same exponent, from ~ 1.1 to ~ 1.7 (or for the stress drops/durations, from ~ 1.15 to ~ 1.5). The relative drift of the cut-off exponent is fully controlled by the same mechanism that controls the drift of τ, since it represents the onset of the system-spanning events (that appear in the hump of the distribution) and leads to off-critical system behavior. We should note that the energy drops is a feature that we cannot predict in our current model approach since it does not include an explicit energy functional that is minimized. The distinction between energy, strain and stress jumps is not transparent in the current model. There are ways to study models that use energy functionals, making simulations more expensive [37], and this is a direction that shall be pursued. It is worth noting that the *super*-linear system size dependence of the avalanche cutoff in our model is clearly connected to the onset of shear-band formation. While in Ref. [17] there is no mention of this shear-banding connection, more recent simulations [18] indicate that the inclusion of inertial effects in particle based dynamics has an even more stringent effect on the steady-state behavior, and it makes the plastic flow curves non monotonous, which for a large system are typically ex-

pected to result in strain localization.

The model studied in this work includes two distinct forms of dynamics that are intertwined through the formation of discrete, abrupt events or avalanches. Experimentally, there is a lot to be said about relaxation properties of disordered solids and glasses, but it is generally well understood that two types of relaxation modes exist: the α-relaxation modes activated at the glass transition temperature and the β-relaxation modes activated at a somewhat lower than the glass transition temperature. While still unclear [45], there is a correlation of the former (α) with large-particle, spatially correlated, slow motions, while the latter (β) associate with small-particle, fast and relatively uncorrelated slip. In the model of this paper, STZ slip dynamics obviosuly corresponds to β-relaxations while slow, viscous relaxation after the fast slip can be thought to correspond to α-like relaxations. The strong effect of fluidity D on the capacity of the system towards shear-banding flows can be thought as the fragility parameter, signifying the dependence of the inverse relaxation time for the α-relaxation modes on temperature ($m = d\ln(\tau_\alpha)/d\ln(T/T_g)$).

In addition, one can understand the analogy between existing models of glasses under shear by considering the basic phenomenology of granular systems under shear. For example, in the case of hard-disks under shear, the expectation is that the contact number locally displays a strong fluctuation with time, in between shear-events. [46]

Our model's distinctive feature is that it contains time-intervals *during* the avalanche process where the pinning potential is locally absent. This mechanism resembles other dynamical weakening mechanisms [37, 41, 42] that function during long *waiting intervals* in-between events, in that there are time intervals where direct minimization of the stress is pursued in a fluid-manner, with no pinning involved. Nevertheless, such dynamics is active in our model only during avalanche events and is due to the disordered nature of the microstructure, while previous efforts focused on thermal relaxations (structural in nature) competing with avalanches to minimize elastic interactions. In comparison to the current model, static frictional stick-slip mechanisms appear similar (both mechanisms assume that after local slip, pinning barriers drop), but lead to apparently different phenomenology, as demonstrated in this manuscript. Differences are due to two key ingredients: i) the capacity of the system to locally seek the true stress minimum (aside from local barriers) for a small but finite timescale T_{pd}, ii) the fact that local slip during time T_{pd} takes the system farther away from the local depinning threshold, albeit after having built collective, self-organized, correlations with the rest of the system.

Finally, we would like to discuss connections of our modelling approach with typical free-volume models. In such theories [47], based on associated self-evident experimental evidence, there is a suggestion that free-volume increase happens at short times (dilation) during shear, while there is slow decrease at longer times. A typical model of the type suggests,

$$\frac{d\epsilon}{dt} \propto c_f \sigma \tag{3}$$

where c_f is the flow defect density, while σ is the stress, which in constitutive models it is assumed to be external; for our purposes this is the stress felt by a single STZ excitation, locally. Following the experimental analysis of disordered solids, it is clear that c_f has a non-trivial evolution in time, where the onset of a strain-rate leads to a defect creation rate $dc_f/dt \sim c_f(\ln c_f)^2\dot{\epsilon}$ while then, the defect concentration tend to decay towards its "equilibrium" value $dc_f/dt \propto -c_f(c_f - c_{eq})$. It is clear, that this physical picture aims to apply inside a single STZ of our model. Namely, one should consider that $f_p \propto 1 - c_f \equiv$(concentration of non-flowing defects) in the large enough STZ. Then, f_p has a creation rate $df_p/dt \propto c_f(c_f - c_{eq})$ and a destruction rate that takes place just after yielding $df_p/dt \propto -c_f(\ln c_f)^2\dot{\epsilon}$ with $c_f \propto 1 - f_p$. This model has a very similar structure to the model solved in this paper, however it is more realistic and should be solved in a separate work, in comparison to existing experiments. Such a model can be interpreted in terms of our construction in the following way: The model of this paper is based on a simple version of the STZ modeling, where the effective temperature dynamics is intrinsically encoded in the dynamics of deformed regions. However, in the context of such phenomenology it is natural to expect that free-volume modeling applies to the length scale below the size of a single STZ, and consequently to timescales close to the time unit, exactly as we discussed.

Experimentally, to our knowledge, there are no well accepted estimates for the critical exponents in avalanche behaviors for disordered solids, such as BMGs or granular/colloidal systems. However, there are several promising experiments that render support to our results. De Richter *et al.* [5] in studies of sandpile avalanches at an incline observed a set of quasi-periodic bursts in addition to an apparent exponent drift for τ, if compared to typically suggested exponent values [28]. Further, Fall *et al.* [7] reported discontinuous slip band formation in colloidal systems with controlled increasing thixotropy. Also, the typical behavior of BMGs where slip band formation appears easier [13] at higher temperatures (where viscosity is lower) and smaller deformation rates (allowing for full relaxation during events), as naturally expected in our construction. While in support of our results, further experiments are needed to clarify the leading mechanisms for slip band formation and avalanches in disordered solids under shear, especially under controlled conditions such as colloidal systems with increasing thixotropy [7] or variable interaction range [40]. In summary of our model's contribution to the phenomenology and experiments, we believe to provide several important clues for the origin of shear-banding in disordered solids: First, our model represents a novel phenomenological interpretation of free-

volume fluctuations in disordered solids in the language of interface depinning modeling. [10]. Second, it may provide alternative explanations for the rate-dependence of shear-banding at low rates [12] in terms of a novel mechanism, that of thixotropic aging. Third, it provides an insightful connection between thixotropic-driven shear-banding and shear-banding in disordered solids, such as BMGs or granular solids. Thixotropy, a phenomenon deeply originating into anisotropic/chainy molecules and hard-core effects, might provide us a strong insight in why shear banding emerges in disordered solids.

Acknowledgments

I would like to thank K. Dahmen, D. M. Dimiduk, M. Robbins, J. P. Sethna, D. Vandembroucq, E. Van der Giessen and S. Zapperi for inspiring discussions. S.P. would like to thank DOE-BES for their support under grant #DE-SC00014109.

[1] D. M. Dimiduk, C. Woodward, R. LeSar, and M. D. Uchic, Science **312**, 1188 (2006).
[2] B. A. Sun, H. B. Yu, W. Jiao, H. Y. Bai, D. Q. Zhao, and W. H. Wang, Physical Review Letters **105**, 035501 (2010).
[3] G. Wang, K. C. Chan, L. Xia, P. Yu, J. Shen, and W. H. Wang, Acta Materialia **57**, 6146 (2009).
[4] Z. W. Shan, J. Li, Y. Q. Cheng, A. M. Minor, S. A. Syed Asif, O. L. Warren, and E. Ma, Physical Review B **77**, 155419 (2008).
[5] S. K. de Richter, V. Y. Zaitsev, P. Richard, R. Delannay, G. L. Caër, and V. Tournat, Journal of Statistical Mechanics: Theory and Experiment **2010**, P11023 (2010).
[6] K. A. Dahmen, Y. Ben-Zion, and J. T. Uhl, Nature Physics **7**, 554 (2011).
[7] A. Fall, J. Paredes, and D. Bonn, Physical Review Letters **105**, 225502 (2010).
[8] R. Burridge and L. Knopoff, Bulletin of the Seismological Society of America **57**, 341 (1967).
[9] D. S. Fisher, K. Dahmen, S. Ramanathan, and Y. Ben-Zion, Physical Review Letters **78**, 4885 (1997).
[10] D. S. Fisher, Physics Reports **301**, 113 (1998).
[11] T. Peterfi, Arch. Entwicklungsmech. Org. **112**, 680 (1927).
[12] C. A. Schuh, T. C. Hufnagel, and U. Ramamurty, Acta Materialia **55**, 4067 (2007).
[13] C. Volkert, N. Cordero, E. Lilleodden, A. Donohue, and F. Spaepen, *Size Effects in the Deformation of Materials: Experiments and Modeling* (MRS Symposia Proceedings No 976E (Materials Research Society, Warrendale, PA, 2007), 2007), pp. 0976–EE11–01.
[14] C. Hays, C. Kim, and W. Johnson, Physical Review Letters **84**, 2901 (2000).
[15] T. Hatano, C. Narteau, and P. Shebalin, Scientific reports, **5**, 12280 (2015).
[16] M. L. Falk, and J. S. Langer, Physical Review E 57 (1998) p. 7192.
[17] K. M. Salerno, and M. O. Robbins, Physical Review E, **88**, p.062206 (2013).
[18] A. Nicolas, J.-L. Barrat and J. Rottler, arxiv:1508.06067 (2015).
[19] N. P. Bailey, J. Schiøtz, A. Lemaître, and K. W. Jacobsen, Physical Review Letters **98**, 095501 (2007).
[20] S. Tewari, D. Schiemann, D. J. Durian, C. M. Knobler, S. A. Langer, and A. J. Liu, Physical Review E **60**, 4385 (1999).
[21] M. Talamali, V. Petäjä, D. Vandembroucq, and S. Roux, Physical Review E **84**, 016115 (2011).
[22] D. Vandembroucq and S. Roux, Physical Review B **84**, 134210 (2011).
[23] K. M. Salerno, C. E. Maloney, and M. O. Robbins, Physical Review Letters **109**, 105703 (2012).
[24] N. Friedman, A. T. Jennings, G. Tsekenis, J.-Y. Kim, M. Tao, J. T. Uhl, J. R. Greer, and K. A. Dahmen, Physical Review Letters **109**, 095507 (2012).
[25] K. A. Dahmen, Y. Ben-Zion, and J. T. Uhl, Physical Review Letters **102**, 175501 (2009).
[26] C. P. Prado and Z. Olami, Physical Review A **45**, 665 (1992).
[27] M. J. Alava, P. K. Nukala, and S. Zapperi, Advances in Physics **55**, 349 (2006).
[28] K. A. Dahmen, Y. Ben-Zion, and J. T. Uhl, Nature Physics **7**, 554 (2011).
[29] R. Maimon and J. Schwarz, Physical Review Letters **92**, 255502 (2004).
[30] J. Schwarz and D. S. Fisher, Physical Review Letters **87**, 096107 (2001).
[31] P. Le Doussal, A. Petković, and K. J. Wiese, Phys. Rev. E **85**, 061116 (2012).
[32] J. D. Eshelby, Proceedings of the Royal Society of London. Series A. Mathematical and Physical Sciences **241**, 376 (1957).
[33] Z. Budrikis, and S. Zapperi, Journal of Statistical Mechanics: Theory and Experiment, 2013(04), p.P04029.
[34] Z. Budrikis and S. Zapperi, arXiv preprint arXiv:1307.2135 (2013).
[35] S. Papanikolaou (in preparation).
[36] Y.-J. Chen, S. Papanikolaou, J. P. Sethna, S. Zapperi, and G. Durin, Phys. Rev. E **84**, 061103 (2011).
[37] S. Papanikolaou, D. M. Dimiduk, W. Choi, J. P. Sethna, M. D. Uchic, C. F. Woodward, and S. Zapperi, Nature **490**, 517 (2012).
[38] K. Martens, L. Bocquet, and J.-L. Barrat, Soft Matter **8**, 4197 (2012).
[39] E. A. Jagla, Physical Review E **76**, 046119 (2007).
[40] H. Guo, S. Ramakrishnan, J. L. Harden, and R. L. Leheny, The Journal of chemical physics **135**, 154903 (2011).
[41] E. A. Jagla, Physical Review E **81**, 046117 (2010).
[42] A. Dobrinevski, P. Le Doussal, and K. J. Wiese, Physical Review E **88**, 032106 (2013).
[43] M. C. Marchetti, A. A. Middleton, and T. Prellberg, Physical Review Letters **85**, 1104 (2000).
[44] S. Papanikolaou, F. Bohn, R. L. Sommer, G. Durin,

S. Zapperi, and J. P. Sethna, Nature Physics **7**, 316 (2011).
[45] Hai Bin Yu, Wei Hua Wang, Hai Yang Bai, and Konrad Samwer, National Science Review **00**,1 (2014).
[46] S. Papanikolaou, C. S. O'Hern, and M. D. Shattuck, Phys. Rev. Letters **110**, (2013) p. 198002.
[47] M. Heggen, F. Spaepen and M. Feuerbacher, Journal of Applied Physics **97**, 033506 (2005).
[48] We note that while there are attempts to model viscous effects [43], the approach used heavily relied on conventional calculus manipulations, even though near the depinning transition the dynamical equations are known to be intrinsically stochastic. Please see Refs. [31, 44] and references therein.
[49] This is not the only option for introducing a cut-off in the simulations [21, 44], but it is appropriate for making contact with experimental results and simulations, given that we investigate the internal timescale structure of the model. Explicit comparison between models lies beyond the purpose of this work.